Mathematical modelling of Love waves propagation in viscoelastic waveguide loaded with complex fluids

Florian Billon, Adil El Baroudi

Mathematical Modelling of Love waves propagation in viscoelastic waveguide loaded with complex fluids

F. Billon[a], A. El Baroudi[a,*]

[a]*LAMPA, Arts et Metiers Institute of Technology, 2 bd du Ronceray, 49035 Angers, France*

Abstract

Love waves propagation in a viscoelastic waveguide loaded on its surface with viscoelastic fluids of finite thickness is investigated in this paper. The Maxwell and Kelvin-Voigt constitutive equations are employed in order to describe the fluid viscoelasticity. By solving the equations of motion in the different media (viscoelastic fluid, viscoelastic waveguide and elastic substrate) and imposing the suitable boundary conditions, an accurate and simple generalized complex dispersion equation is established for Love waves. Subsequently, a comparison is made with the published complex dispersion equations in the literature in some particular cases, and a very good agreement is showed. A detailed study was conducted by varying key parameters such as operating frequency, waveguide thickness and fluid thickness. The waveguide surface was subjected to various glycerol concentrations, with a wide range of dynamic viscosity, representing both Newtonian and viscoelastic behaviors. Theoretical analysis shows that to reasonably predict the characteristics responses of Love waves, the Maxwell fluid is more appropriate for low glycerol concentration and, the Kelvin-Voigt fluid is more suitable for high glycerol concentration and at high frequency. Results also evaluated the influence of layer thickness on the dispersion curves. The obtained results can be very useful in the design and optimization of Love wave fluid sensors.

Keywords: Love wave, Viscoelastic fluid, Viscoelastic waveguide, Analytical modeling.

*Corresponding author

Email address: adil.elbaroudi@ensam.eu (A. El Baroudi)

1. Introduction

There is an increasing demand of highly sensitive analytical techniques in the fields of biotechnology [1], medical diagnostics [2] and chemistry [3]. Optical and acoustic waves sensing technologies are currently used [4]. In particular, the Love wave acoustic sensors have attracted increasing attention from the scientific community during the last two decades, due to their reported high sensitivity in liquid. Love wave is a transverse surface wave having one component of mechanical displacement, which is parallel to the surface and perpendicular to the direction of wave propagation. The Love wave sensor is a layered structure formed by a piezoelectric substrate and a guiding layer [5, 6, 7]. In addition, the condition for the existence of Love waves is that the bulk transverse wave velocity in the layer is lower than that in the substrate. The difference between the mechanical properties of the guiding layer and the substrate creates an entrapment of the acoustic energy in the guiding layer keeping the wave energy near the surface [8]. The confinement of the wave in the guiding layer makes Love wave devices very sensitive towards any changes occurring on the sensor surface [9].

The interaction with a viscous fluid was firstly studied in 1992. An exact solution was used to correlate the velocity and attenuation with the fluid viscosity [10, 11]. This article describes a detailed analytical study to predict the propagation of Love wave in viscoelastic waveguide loaded on its surface with a viscoelastic fluid. In this study we will determine how the characteristics of Love waves are affected by loading viscoelastic fluids with finite thickness. These characteristics are very important in a design and optimization of Love wave fluid sensors. To date, the theory of Love wave propagation has been developed for elastic waveguide loaded on the surface with the Newtonian fluid [6, 12], and elastic waveguide loaded on the surface with the Maxwell fluid [13]. In the present work, we investigate a more general situation, i.e. we consider a case in which the viscoelasticity of fluid and waveguide is taken into account. To this end, the coupled differential problem which describes the propagation of the Love wave in the viscoelastic waveguide structure loaded on its surface with viscoelastic fluids (see Figure 1) was formulated and solved analytically. Love wave fluid sensors can be used to determine the viscosity of various fluids processed in the plastics and chemical industries. Moreover, the obtained dispersion equation can be very useful in nondestructive investigations of composite materials in order to interpret the obtained experimental measurements.

2. Physical model description

To describe the waveguide structure that guides Love waves, we consider a three-layer system consisting of a viscoelastic fluid (index f), a viscoelastic elastic surface layer (i.e. waveguide, index v) and an elastic solid substrate (index e), see Figure 1. The waveguide is designed to support shear horizontal surface waves of the Love type. The waveguide structure consists of a viscoelastic layer ($0 < x_2 < h_v$), which is rigidly bonded to a semi-infinite elastic substrate occupying the lower half-space ($x_2 > h_v$). In addition, top of the surface layer of the waveguide ($x_2 = 0$) is loaded with a viscoelastic fluid ($-h_f < x_2 < 0$) of finite thickness h_f. All material parameters of the waveguide structure change only along the x_2 axis. Love surface waves have only one non zero shear horizontal component of the mechanical displacement u_3, which is directed along the x_3 axis, parallel to the surface ($x_2 = 0$) of the waveguide and perpendicular to the direction of the Love wave propagation along the x_1 axis. Note that the Love waves exhibit a multimode character, the fundamental mode plays an important role in many application such as non destructive testing and sensors [11]. Accordingly, in this work, the attention is focused on the properties of the fundamental mode of Love waves. In addition, losses in the viscoelastic waveguide are considered.

From the experimental point of view, phase and amplitude characteristics of Love surface waves can be measured in a closed loop configuration by placing Love wave delay line in a feedback circuit of an electrical oscillator. Another possibility is to use a network analyzer. This apparatus provides phase shift and insertion loss of the Love wave sensor due to the load of the sensor with a measured viscoelastic fluid. The typical frequency range used by Love wave sensors is from 50 MHz to 500 MHz [14].

2.1. Viscoelastic waveguide

In this section, we derive the differential equations describing wave propagation in terms of the displacements of the material using continuum mechanics. The conservation of linear momentum in the absence of the body forces implies [15]

$$\rho_v \frac{\partial^2 \mathbf{u}^{(v)}}{\partial t^2} = \nabla \cdot \boldsymbol{\sigma}^{(v)} \tag{1}$$

where $\mathbf{u}^{(v)}$ is the displacement vector, ρ_v is the density and $\boldsymbol{\sigma}^{(v)}$ is the total stress tensor. A viscoelastic model commonly used to describe anelastic effects is the Kelvin-Voigt stress-strain relation, which consists of a spring

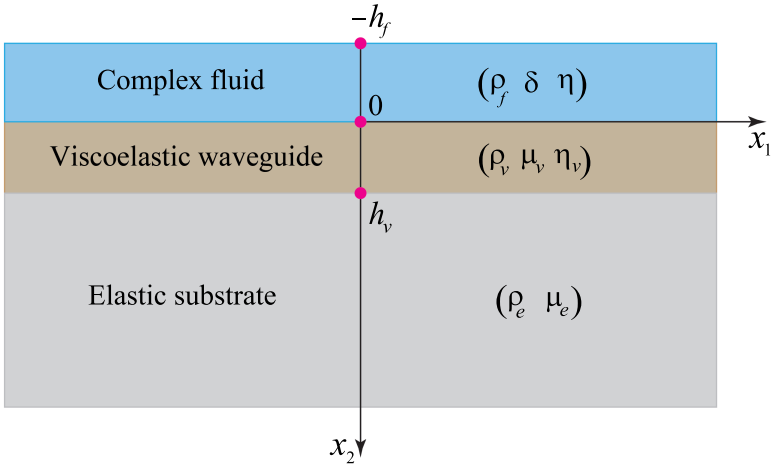

Figure 1: The model geometry. The surface layer (index v) is viscoelastic medium and the substrate (index e) is elastic medium. ρ_v, μ_v and η_v correspond to the density, shear modulus and viscosity of the viscoelastic layer. ρ_e and μ_e the density and shear modulus of the elastic substrate. The viscoelastic surface layer is loaded by a viscoelastic fluid. Love wave propagates in the x_1-direction and displacement in the x_3-direction. For viscoelastic fluid, ρ_f, η and δ are, respectively, density, dynamic viscosity and relaxation time.

and a dashpot connected in parallel. Therefore, the total stress is composed of an elastic stress and a viscous stress as follow [16]

$$\boldsymbol{\sigma}^{(v)} = 2\mu_v \boldsymbol{\varepsilon}^{(v)} + 2\eta_v \frac{\partial \boldsymbol{\varepsilon}^{(v)}}{\partial t} \tag{2}$$

where μ_v is the storage shear modulus (spring constant), η_v is the viscosity of the viscoelastic layer (dashpot constant), and $\boldsymbol{\varepsilon}^{(v)} = \left\{\nabla \mathbf{u}^{(v)} + \left[\nabla \mathbf{u}^{(v)}\right]^T\right\}/2$ is the total strain of the system.

The Love wave is taken to propagate in the x_1-direction, with shear displacement in the x_3-direction. A plane wave in the x_1-direction is considered, with displacement in x_3-direction only, $\mathbf{u}^{(v)} = \left(0, 0, u_3^{(v)}\right)$. Owing to symmetry, the mechanical displacement should be independent of x_3, $u_3^{(v)} = u_3^{(v)}(x_1, x_2)$. Applying the divergence operator to both sidesof Eq. (2) and taking into account Eq. (1), we get the following viscoelastic waveguide equation expressed in terms of the component of the displacement along the x_3 axis

$$\mu_v \nabla^2 u_3^{(v)} + \eta_v \frac{\partial}{\partial t} \nabla^2 u_3^{(v)} - \rho_v \frac{\partial^2 u_3^{(v)}}{\partial t^2} = 0 \tag{3}$$

where ∇^2 is the Laplacian operator in Cartesian coordinates.

2.2. Elastic substrate

In this work the substrate is considered to be a semi-infinite medium [13, 17], and mechanical displacement $u_3^{(e)}$ is governed, using the elastodynamic theory by the Navier's equation [15]

$$\mu_e \nabla^2 u_3^{(e)} - \rho_e \frac{\partial^2 u_3^{(e)}}{\partial t^2} = 0 \tag{4}$$

where μ_e is the storage shear modulus and ρ_e the density. Note that Eq. (4) can easily be obtained by setting $\eta_v = 0$ in Eq. (3).

2.3. Viscoelastic fluid

The fluid occupying $-h_f < x_2 < 0$ is assumed to be viscoelastic and nonconductive. To describe the viscoelasticity of the fluid, the Maxwell and Kelvin-Voigt models are employed. The Maxwell model introduces the viscoelastic response of the fluid at high frequencies and that of Kelvin-Voigt at low frequencies. The Maxwell model consists of a spring and a damper connected in series. The damper represents energy losses and is characterized by the viscosity η, whereas the spring represents the energy storage and is characterized by the elastic shear modulus μ. These two quantities are related through the relaxation time $\delta = \eta/\mu$, which is the characteristic time for the transition between viscous and elastic behavior [18]. Thus, suppose the motion of the fluid is induced only by wave propagation in the waveguide material and also propagates in the form of a harmonic wave. Therefore, the governing equation for the fluid is described by the Cauchy's equation :

$$\rho_f \left[\frac{\partial \mathbf{v}}{\partial t} + (\mathbf{v} \cdot \nabla)\, \mathbf{v} \right] = -\nabla p + \nabla \cdot \boldsymbol{\tau} \tag{5}$$

where ρ_f is the density, $\mathbf{v}$ is the velocity vector, p is the pressure and $\boldsymbol{\tau}$ is the shear stress tensor. Therefore, the constitutive equations which relate the shear stress tensor to deformation are [20]

$$\boldsymbol{\tau} + \delta \frac{\partial \boldsymbol{\tau}}{\partial t} = 2\eta \mathbf{D} \tag{6}$$

$$\frac{\partial \boldsymbol{\tau}}{\partial t} = 2\mu \mathbf{D} + 2\eta \frac{\partial \mathbf{D}}{\partial t} \tag{7}$$

where $\mathbf{D} = \left[\nabla\mathbf{v} + (\nabla\mathbf{v})^T\right]/2$ is the strain rate tensor. The stress-strain relation (6) is suggested by Maxwell for the characterization of viscous fluids with elastic properties, and the stress-strain relation (7) is proposed by Kelvin-Voigt for the description of elastic solids with viscous properties. Similarly the mechanical displacement, since a plane wave in the x_1-direction is considered, with displacement in x_3-direction only, the velocity field can be expressed as $\mathbf{v} = [0, 0, v_3(x_1, x_2)]$. Moreover, the pressure gradient can also be ignored since only shear deformation occurs during wave propagation [19]. In regard to this problem, the inertial term in the Cauchy's equation (5) can be neglected. Therefore, applying the divergence operator to both sides of Eqs. (6) and (7), and taking into account the Eq. (5), we get the following viscoelastic fluid equation expressed in terms of the axial component v_3 of the velocity field

$$\nabla^2 v_3 - \frac{\rho_f}{\eta}\left(\frac{\partial v_3}{\partial t} + \delta\frac{\partial^2 v_3}{\partial t^2}\right) = 0 \tag{8}$$

$$\nabla^2 v_3 + \delta\frac{\partial}{\partial t}\nabla^2 v_3 - \frac{\delta\rho_f}{\eta}\frac{\partial^2 v_3}{\partial t^2} = 0 \tag{9}$$

Equation (8) describes the fluid motion according to the Maxwell behavior and Eq. (9) to that of Kelvin-Voigt behavior. The solution of these equations and those of equations (3) and (4) are to be substituted in the relevant boundary conditions.

2.4. Analytical solutions for the equations of motion

A general plane harmonic wave solution for the equations of motion (3), (4), (8) and (9) is sought in the following form :

$$\begin{Bmatrix} u_3^{(v)} \\ u_3^{(e)} \\ v_3 \end{Bmatrix}(x_1, x_2, t) = \begin{Bmatrix} U_v(x_2) \\ U_e(x_2) \\ V(x_2) \end{Bmatrix} e^{j(kx_1 - \omega t)} \tag{10}$$

where ω represents the angular frequency. Love wave propagating in the viscoelastic layer undergoes attenuation, hence, the wavenumber k along the propagation direction of the Love wave becomes complex, $k = k_r + jk_i$, the real part k_r determines the Love wave velocity, the imaginary part k_i, is the Love wave attenuation. Moreover, the x_2 dependence represents the distribution of the mechanical displacement and velocity as a function of

depth x_2. Substitution of Eq. (10) into Eqs. (3), (4), (8) and (9) gives rise to the following differential equations of the second order :

$$\begin{array}{l} U_v''(x_2) + \beta_v^2 U_v(x_2) = 0 \\ U_e''(x_2) - \beta_e^2 U_e(x_2) = 0 \\ V''(x_2) - \beta_f^2 V(x_2) = 0 \end{array} \tag{11}$$

where the wavenumbers β_v, β_e and β_f are given in the following form

$$\beta_v = \sqrt{\frac{\omega^2}{c_v^2 - \frac{j\omega\eta_v}{\rho_v}} - k^2}\ , \quad \beta_e = \sqrt{k^2 - \frac{\omega^2}{c_e^2}}\ , \quad \beta_f = \sqrt{k^2 - \frac{j\omega\rho_f}{\eta^*}} \tag{12}$$

and $c_v = \sqrt{\mu_v/\rho_v}$ and $c_e = \sqrt{\mu_e/\rho_e}$ are the shear waves velocities in the layer and substrate, respectively. The complex dynamic viscosity η^* present in the fluid wavenumber β_f can be defined according to the used viscoelastic fluid behavior as

$$\eta^* = \begin{cases} \dfrac{\eta}{1 - j\mathrm{De}} & \text{for Maxwell fluid} \\ \eta - \dfrac{\eta}{j\mathrm{De}} & \text{for Kelvin-Voigt fluid} \end{cases} \tag{13}$$

where $\mathrm{De} = \omega\delta$ is the Deborah number. Note that when $\mathrm{De} \ll 1$ (Maxwell fluid), or $\mathrm{De} \gg 1$ (Kelvin-Voigt fluid), the fluid exhibits a purely Newtonian (viscous) behavior and the fluid wavenumber β_f becomes $\xi = \sqrt{k^2 - j\omega\rho_f/\eta}$. Since the amplitude of Love surface waves must tend to zero for $x_2 \to \infty$, the solution of Eq. (11) can be written in the form of

$$\begin{array}{l} U_v(x_2) = A_v \cos(\beta_v x_2) + B_v \sin(\beta_v x_2) \\ U_e(x_2) = A_e e^{-\beta_e x_2} \\ V(x_2) = A_f e^{-\beta_f x_2} + B_f e^{\beta_f x_2} \end{array} \tag{14}$$

where A_v, B_v, A_e, A_f and B_f are unknown arbitrary amplitudes.

2.5. Boundary conditions

The solution of the Love wave propagation must satisfy the boundary conditions on the fluid ($x_2 = -h_f$), the continuity conditions along the interface between the waveguide layer and the fluid ($x_2 = 0$), and between the substrate and the waveguide layer ($x_2 = h_v$). At the interface $x_2 = 0$,

the mechanical conditions are continuity of displacement, velocity and stress components, i.e.

$$v_3 = \frac{\partial u_3^{(v)}}{\partial t} \ , \quad \tau_{23} = \sigma_{23}^{(v)} \tag{15}$$

The surface of the fluid is open boundary ($x_2 = -h_f$). This requires

$$\tau_{23} = 0 \tag{16}$$

At the interface $x_2 = h_v$, the mechanical conditions are continuity of displacement and stress components, i.e.

$$u_3^{(v)} = u_3^{(e)} \ , \quad \sigma_{23}^{(v)} = \sigma_{23}^{(e)} \tag{17}$$

Furthermore, the shear stress component displacement that will be used in these boundary conditions are given by

$$\sigma_{23}^{(v)} = (\mu_v - j\omega\eta_v) \frac{\partial u_3^{(v)}}{\partial x_2} \ , \quad \sigma_{23}^{(e)} = \mu_e \frac{\partial u_3^{(e)}}{\partial x_2} \ , \quad \tau_{23} = \eta^* \frac{\partial v_3}{\partial x_2} \tag{18}$$

2.6. Complex dispersion equation

Substitution of the Eqs. (10) and (18) into the boundary conditions (15)-(17) yields a system of five linear algebraic equations in five undetermined amplitudes. For nontrivial solutions of the undetermined amplitudes to exist, the determinant of this system has to equal zero, which leads to the following dispersion equation of the Love waves :

$$\frac{j\omega\eta^*\beta_f}{\beta_v (\mu_v - j\omega\eta_v)} \tanh(\beta_f h_f) + \frac{\beta_v (\mu_v - j\omega\eta_v) \tan(\beta_v h_v) - \mu_e \beta_e}{\mu_e \beta_e \tan(\beta_v h_v) + \beta_v (\mu_v - j\omega\eta_v)} = 0 \tag{19}$$

Since this relation contains k, ω, as well as all material and geometrical parameters of the viscoelastic fluid, viscoelastic waveguide and elastic substrate, Eq. (19) represents the implicit complex dispersion equation of Love waves propagating in a viscoelastic waveguide loaded with a viscoelastic fluid. Eq. (19) was solved using Mathematica software. Once the wavenumber is obtained, the phase velocity is calculated by $v_p = \omega / k_r$. While the imaginary part of wavenumber k_i represents the attenuation per unit length in the propagation direction. Furthermore, the Deborah number De present in the complex dynamic viscosity η^* depends both on ω and δ. The three following regimes may be highlighted in the case of :

- Maxwell fluid: (i) For De $\ll 1$ the oscillation time $(= 1/\omega)$ is greater than the relaxation time and, the fluid exhibits a purely viscous behavior. (ii) For De $\gg 1$ the oscillation time is smaller than the relaxation time and, the fluid exhibits an elastic behavior. (iii) For De $= 1$ the transition from Newtonian to Maxwell regime takes place.

- Kelvin-Voigt fluid: (i) For De $\ll 1$ the oscillation time is greater than the relaxation time and, the fluid exhibits an elastic behavior. (ii) For De $\gg 1$ the oscillation time is smaller than the relaxation time and, the fluid exhibits a purely viscous behavior. (iii) For De $= 1$ the transition from Newtonian to Kelvin-Voigt fluid regime takes place.

2.7. Some particular cases

For the special case when $h_f \to \infty$ (semi-infinite viscoelastic fluid), the complex dispersion equation (19) becomes

$$j\omega\eta^*\beta_f - \mu_e\beta_e + \left[\frac{j\omega\eta^*\beta_f\mu_e\beta_e}{\beta_v\left(\mu_v - j\omega\eta_v\right)} + \beta_v\left(\mu_v - j\omega\eta_v\right)\right]\tan\left(\beta_v h_v\right) = 0 \qquad (20)$$

Moreover, if the Maxwell fluid is considered and assuming an elastic waveguide (i.e. $\eta_v = 0$), the complex dispersion equation (20) takes the following form

$$\mu_v\beta_v\left(\frac{j\omega\eta\beta_f}{1 - j\mathrm{De}} - \mu_e\beta_e\right) + \left(\frac{j\omega\eta\beta_f}{1 - j\mathrm{De}}\mu_e\beta_e + \mu_v^2\beta_v^2\right)\tan\left(\beta_v h_v\right) = 0 \qquad (21)$$

which was previously obtained by [13]. In addition, for a Newtonian fluid, the complex dispersion equation (21) can be rearranged to give

$$\mu_v\beta_v\left(j\omega\eta\xi - \mu_e\beta_e\right) + \left(j\omega\eta\xi\mu_e\beta_e + \mu_v^2\beta_v^2\right)\tan\left(\beta_v h_v\right) = 0 \qquad (22)$$

which was previously obtained by [6, 13, 21]. A last comparison can be drawn between the present generalized complex dispersion equation (19) and those of literature in the case of Love waves propagating in viscoelastic waveguide without any fluid on its surface. Therefore, the complex dispersion equation (19) becomes :

$$\beta_v\left(\mu_v - j\omega\eta_v\right)\sin\left(\beta_v h_v\right) - \mu_e\beta_e\cos\left(\beta_v h_v\right) = 0 \qquad (23)$$

which was previously obtained by [22].

3. Comparison with other studies

In this paragraph, we check the accuracy and numerical robustness of the dispersion equation developed in this work in some particular cases. Firstly, a comparison study is performed for a viscoelastic waveguide without a fluid loaded on its surface. To compare the results derived from the equation (19) with other theoretical established results, the same dimensionless parameters that were used by Kielczynski [22] are introduced. Figure 2 illustrates the dispersion curves of the Love wave attenuation as function of waveguide thickness. Figure 2 shows a non monotonic behavior of the Love wave attenuation with the waveguide thickness. Indeed, the attenuation has a pronounced maximum as a function of waveguide thickness. For increasing frequencies of the Love wave the maximum occurs for lower thicknesses of the waveguide, i.e., for frequencies $f = 100, 200$ and $300\,\mathrm{MHz}$ the maximum occurs, respectively, for $h_v = 2.9, 1.46$ and $0.97\,\mu\mathrm{m}$. Moreover, when the frequency increases, the Love wave attenuation is stronger. In addition, the results in the Figure 2 agree exceptionally well with those obtained by Kielczynski [22].

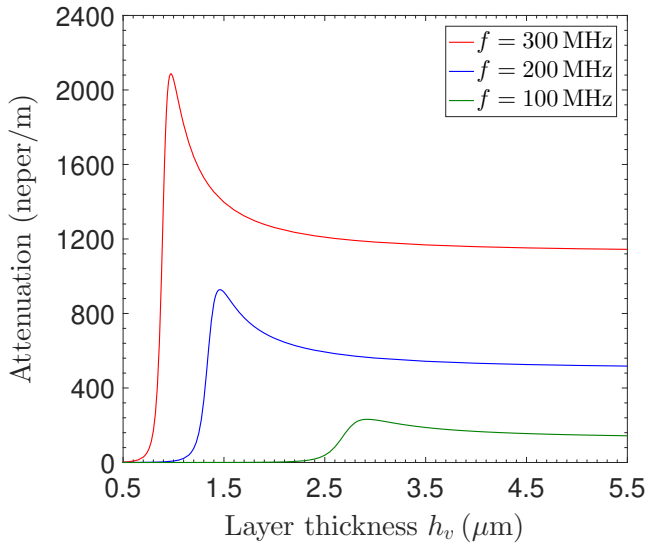

Figure 2: Love wave attenuation versus the layer thickness without fluid loading in the case of a viscoelastic waveguide ($\eta_v = 10^{-3}\,\mathrm{Pa}\cdot\mathrm{s}$). This Figure is identical to that of Ref. [22].

A second and last comparison can be drawn between the present dispersion equation and that of Kielczynski et al. [12] in the case of an elastic waveguide, loaded with a Newtonian liquid layer of finite thickness. Variations of Love wave attenuation versus liquid layer thickness are investigated. If the Newtonian liquid thickness h_f is finite, a strong dependence of the attenuation on the actual value of h_f is observeed in the Figure 3. Initially, for the thickness h_f of the loading Newtonian liquid growing from zero the attenuation increases monotonically and reaches a maximum for the thickness h_f equaled approximatelly to the fluid penetration depth [27] defined as $d = \sqrt{2\eta_f/\rho_f\omega}$ ($h_f \approx d$). Increasing further the thickness $h_f > d$, we observe that the attenuation drops monotonically and attains a local minium at $h_f \approx 2d$. Next, (for $h_f \approx 2d$) the attenuation slightly grows and enters a plateau for $h_f \approx 4d$. It means that if thickness of the Newtonian liquid is $h_f \approx 4d$, we can consider practically such a layer of Newtonian liquid as infinite (or semi-infinite). Note that a similar behavior is obtained by Kielczynski et al. [12].

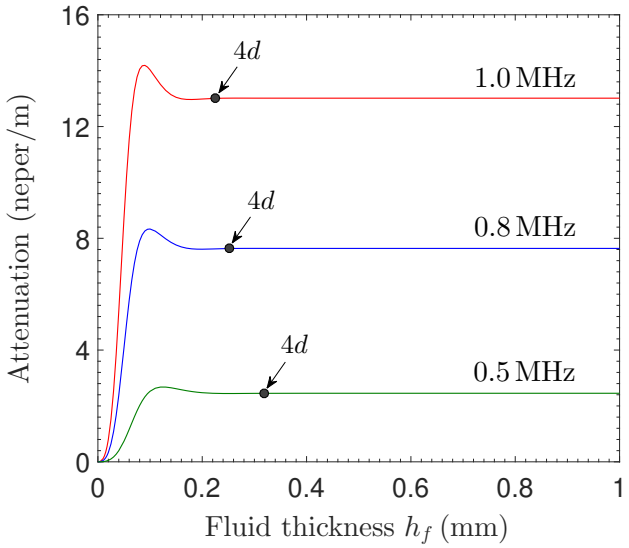

Figure 3: Love wave attenuation versus the fluid thickness in the case of Newtonian fluid ($\eta = 10\,\mathrm{Pa}\cdot\mathrm{s}$) and elastic waveguide (i.e. $\eta_v = 0$) with $h_v = 0.1\,\mathrm{mm}$.

4. Numerical results and discussion

Having established the accuracy through the comparison study illustrated in Figures 2 and 3, further numerical results are given in this section. The material properties given in Table 1 for the viscoelastic waveguide and elastic substrate [22], and in Table 2 for viscoelastic fluids [5], are taken to construct this numerical example. In this work,numerical calculation is performed in the glycerol concentrationsrange from 15.4 to 88.0% and for three values of frequency 50, 100 and 150 MHz.

	Waveguide	Substrate
Shear waves velocity	$c_v = 1100.85\,(\mathrm{m/s})$	$c_e = 5060.02\,(\mathrm{m/s})$
Storage shear modulus	$\mu_v = 1.43\,(\mathrm{GPa})$	$\mu_e = 67.85\,(\mathrm{GPa})$
Density	$\rho_v = 1180\,(\mathrm{kg/m^3})$	$\rho_e = 2650\,(\mathrm{kg/m^3})$

Table 1: Material parameters used for waveguide and substrate.

4.1. Phase velocity and attenuation versus waveguide thickness

Figure 4 shows the plot of the phase velocity and attenuation of the Love wave versus the layer thickness h_v (waveguide thickness), for various waveguide viscosity ($\eta_v = 0.001, 0.01, 0.1\,\mathrm{Pa\cdot s}$) and frequencies ($50, 100, 150\,\mathrm{MHz}$). As it is seen in Figures 4(a) and 4(b) the phase velocity v_p of the Love wave begins at $v_p = c_v$ for $h_v = 0$ and decreases monotonically to the substrate shear wave velocity $v_p = c_e$. In other words, for thicker waveguide surface, properties of the Love wave are more influenced by properties of the substrate. Figures 4(a) and 4(b) show also that the viscosity of the viscoelastic waveguide has insignificant effect on the phase velocity. In contrast to the phase velocity, the attenuation of Love waves depends strongly on viscosity η_v of the viscoelastic waveguide.

The influence of the waveguide thickness on the Love wave attenuation is illustrated in Figures 4(c) and 4(d). These Figures show that the Love wave attenuation k_i has a pronounced maximum as a function of waveguide thickness h_v. For increasing frequencies the maximum occurs for lower thicknesses of the waveguide, i.e., for frequencies $f = 50$ and $100\,\mathrm{MHz}$ the maximum occurs, respectively, for $h_v = 5.7$ and $2.84\,\mu\mathrm{m}$. This maximum was also observed in the case of an elastic waveguide [13]. The obtained curves are similar to those of sensitivity to the mass effect obtained for a Love wave sensor [11]. To interpret these results, the energy confinement

χ (%)	η (mPa $\cdot$ s)	ρ_f (kg/m^3)	δ (ps)
15.4	1.4	1017	28
25.6	1.7	1029	38
32.9	2.7	1038	54
37.3	3.1	1044	62
42.3	3.8	1050	76
46.7	4.6	1055	92
52.2	5.9	1062	118
62.1	10.2	1075	204
72.0	21.9	1087	438
75.9	33.2	1093	664
80.0	49.5	1098	990
84.0	81.8	1104	1636
88.0	128.1	1109	2562

Table 2: Material parameters used for water-glycerol mixtures. χ is the concentration of glycerol in water.

in the waveguide has to be taken into account. Thus, when the waveguide thickness increases, the energy of the Love wave increases while the energy present in the substrate decreases [8]. This has the effect of increasing wave amplitude at the interface with the liquid. The attenuation due to the viscoelastic properties of the liquid thus becomes stronger. To conclude, the maximum of Love waves attenuation as a function of the waveguide thickness is due mainly to the energy confinement in the waveguide. Moreover, the amplitude of this maximum is amplified due to both the fluid viscosity and the viscosity of the waveguide.

4.2. Influence of the glycerol concentration on the Love wave attenuation

In this paragraph, we investigate how the attenuation vary with the glycerol mass fraction (i.e., shear viscosity) in both Newtonian and viscoelastic fluids. Indeed, by considering a viscous fluid and increasing the glycerol mass fraction, a Newtonian fluid predicted a monotonically increasing relationship between the attenuation and the glycerol mass fraction [23]. Figure 5 is in good agreement with this Newtonian behavior. However, the Maxwell and Kelvin-Voigt fluids highlighted a non-monotonically decreasing correlation

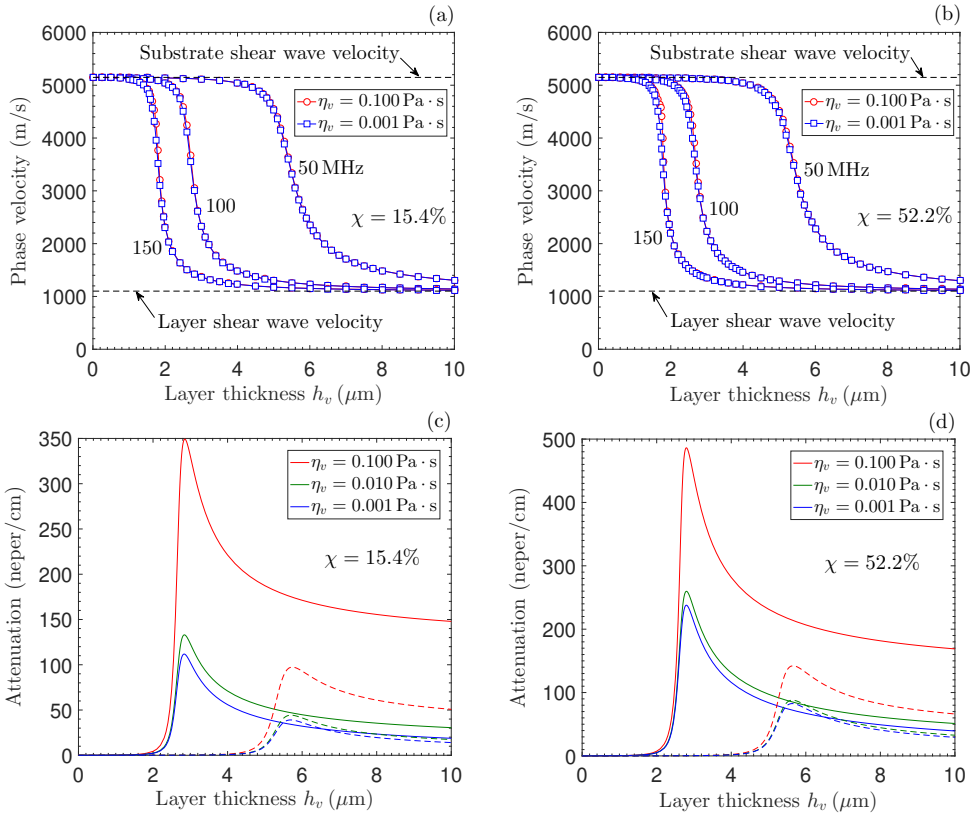

Figure 4: Love phase velocity and attenuation versus the layer thickness in the case of Newtonian fluid ($\chi = 15.4\%$) with $h_f = 20\,\mu$m. In Figures (c) and (d) : dashed lines $f = 50\,$MHz and solid lines $f = 100\,$MHz.

between the attenuation and glycerol mass fraction. Therefore we can conclude that the non-monotonic behavior manifested the intrinsic viscoelastic properties of fluid [24, 25, 26]. In addition, Figure 5(a) shows the attenuation variation for a frequency equal to 50 MHz and for a waveguide thickness of 1 m. In the case of a Maxwell fluid, the elastic effects are significant for a glycerol concentration greater than 62.1%. In other words, for Deborah number values less than the critical values of 0.064, the elasticity can be neglected and the behavior is purely Newtonian. This is due to the time constant value less than 204 ps corresponding to De less than 0.064. The term De is then negligible compared to 1 and the complex dynamic viscosity η^* can be assimilated to the dynamic viscosity η characterizing a Newtonian behavior. Thus, a similar results are obtained for others excitation frequen-

cies and waveguide thickness (see Figure 5). These observations are in good agreement with the literature results [5]. Therefore, to reasonably predict the characteristics responses of Love waves, the Maxwell fluid is more appropriate for low glycerol concentration and, the Kelvin-Voigt fluid is more suitable for high glycerol concentration and at high frequency.

4.3. Love wave attenuation versus frequency

The dependence of the attenuation on the frequency for two values of the glycerol concentration ($\chi = 62.1\%$ and 88.0%) in the case of Newtonian and Maxwell fluids is depicted in Figure 6. As can be seen in this Figure, the attenuation depends strongly on the frequency and glycerol concentration. Whatever the fluid used, with an increase in the frequency and glycerol concentration causes a non monotonic behavior in the Love wave attenuation. It is seen that the attenuation values obtained with the Maxwell model converge towards those obtained with the Newtonian model for frequencies lower than 20 MHz. At about 29 MHz ($\chi = 62.1\%$) and 27 MHz ($\chi = 88.0\%$), the attenuation reaches a local maximum. In spite of the increased viscosity of fluid (increase in glycerol concentration), the attenuation is less pronounced in the case of the Maxwell model due to the elastic behavior of the fluid at high frequencies. Figure 6 also highlights a less important difference between Maxwell curves and those of Newtonian fluid for $\chi = 62.1\%$. In other words, for glycerol concentrations lower than 62.1%, the fluid behaves as Newtonian. However, this difference becomes more important for glycerol concentrations higher than 62.1% and the fluid exhibits a purely elastic behavior from a frequency of 63 MHz. In other words, for frequencies over 63 MHz the mixtures response converges towards an attenuation limit value. It corresponds to the fact that de fluid develops a purely elastic behaviour. If we want to take reference about concrete example, it shows the same behavior as fluid materials that becomes solid when we put it under stress. Note that Nagy and Nayfeh [28] highlight a similar behavior of longitudinal waves attenuation curves in the case of newtonian fluid, even though the vibration mechanism is fundamentally different.

4.4. Phase velocity and attenuation versus fluid thickness

Figure 7 exhibits the plot of Love wave phase velocity and attenuation as a function of fluid thickness, for frequencies $f = 100$ and 150 MHz and two glycerol concentrations $\chi = 62.1$ and 88%. When the fluid thickness h_f is

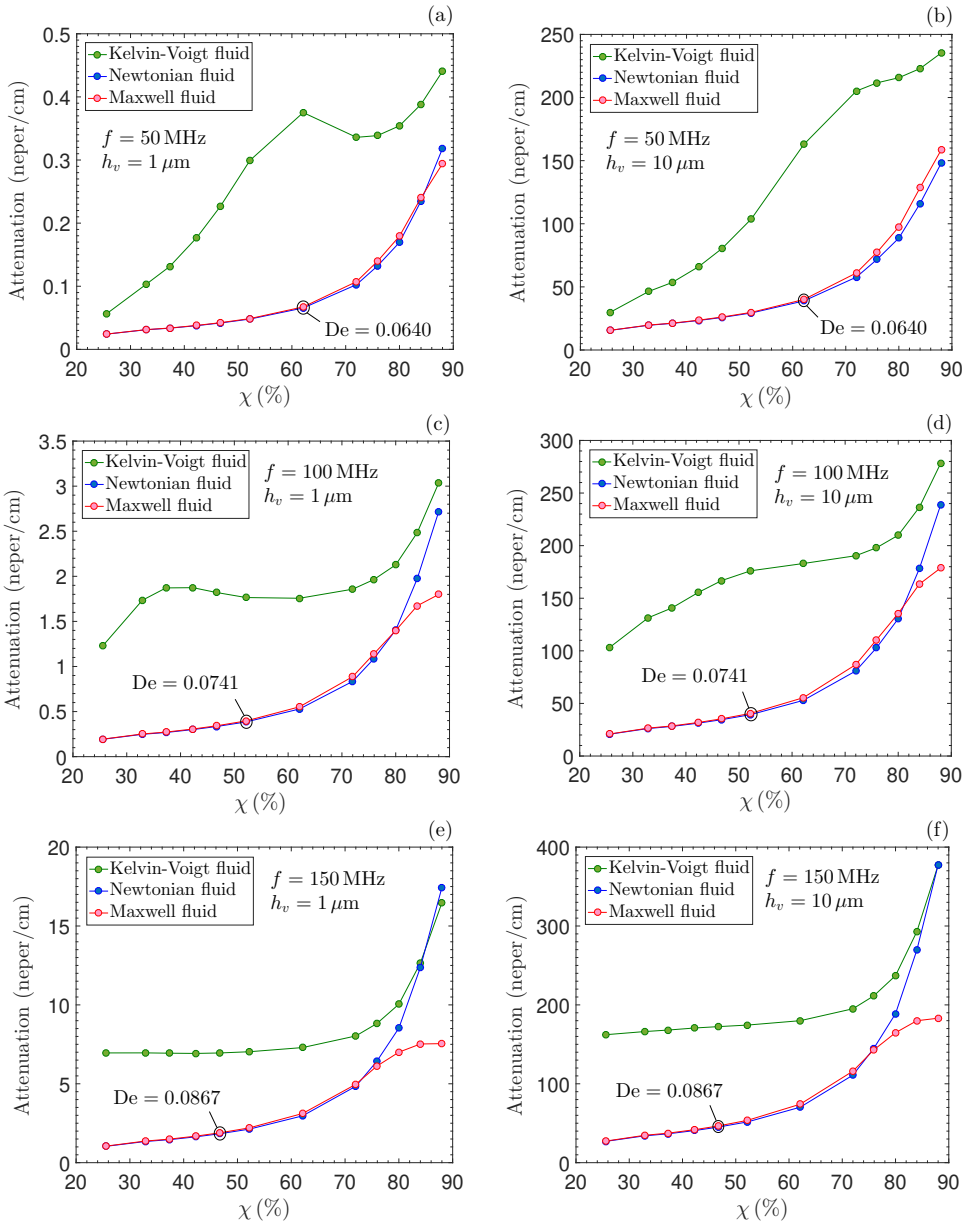

Figure 5: Love wave attenuation versus the glycerol mass fraction with $\eta_v = 1 \times 10^{-3}$Pa $\cdot$ s and $h_f = 20\,\mu$m.

finite, a strong dependence of the Love wave phase velocity and attenuation on the actual value of h_f is observed.

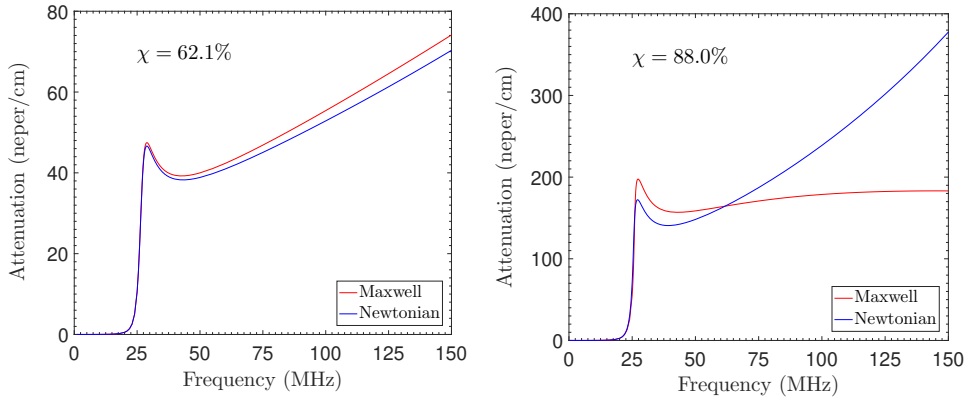

Figure 6: Love wave attenuation versus frequency with $\eta_v = 1 \times 10^{-3}\text{Pa} \cdot \text{s}$, $h_v = 10\,\mu\text{m}$ and $h_f = 20\,\mu\text{m}$.

For example, in the case of a frequency of 100 MHz and a glycerol concentration of $\chi = 62.1\%$, Figure 7(a) shows that, initially, for the fluid thickness growing from zero the phase velocity drops monotonically and reaches a minimum for the thickness h_f equaled to $0.16\,\mu\text{m}$. Increasing further the fluid thickness, we observe that the phase velocity grows monotonically and attains a local maximum at $h_f = 0.4\,\mu\text{m}$. Next, for $h_f > 0.4\,\mu\text{m}$ the phase velocity slightly drops and enters a plateau for $h_f = 4.6d$. In other words, that if the fluid thickness $h_f = 4.6d$, we can consider practically such a fluid layer as infinitive. This is an important result in design of Love wave fluid sensors. Note that a same behavior is observed for other frequencies and glycerol concentrations. However, in the case of attenuation, Figure 7(b) illustrates an opposite behavior to that of the phase velocity. Indeed, initially, for the fluid thickness growing from zero the attenuation increases monotonically and reaches a maximum. Increasing further the thickness, we observe that the attenuation decreases monotonically and attains a local minimum. Next, the attenuation slightly increases and enters a plateau for h_f equaled to the 4.6 times fluid penetration depth. Figure 7 also shows that the value of the plateau strongly depends on the excitation frequency and the used fluid model. Therefore, to accurately optimize the height of the fluid from which it can be assumed to be a semi-infinite medium, the phase velocity and the attenuation must be correctly predicted as function of the fluid model and excitaion frequency.

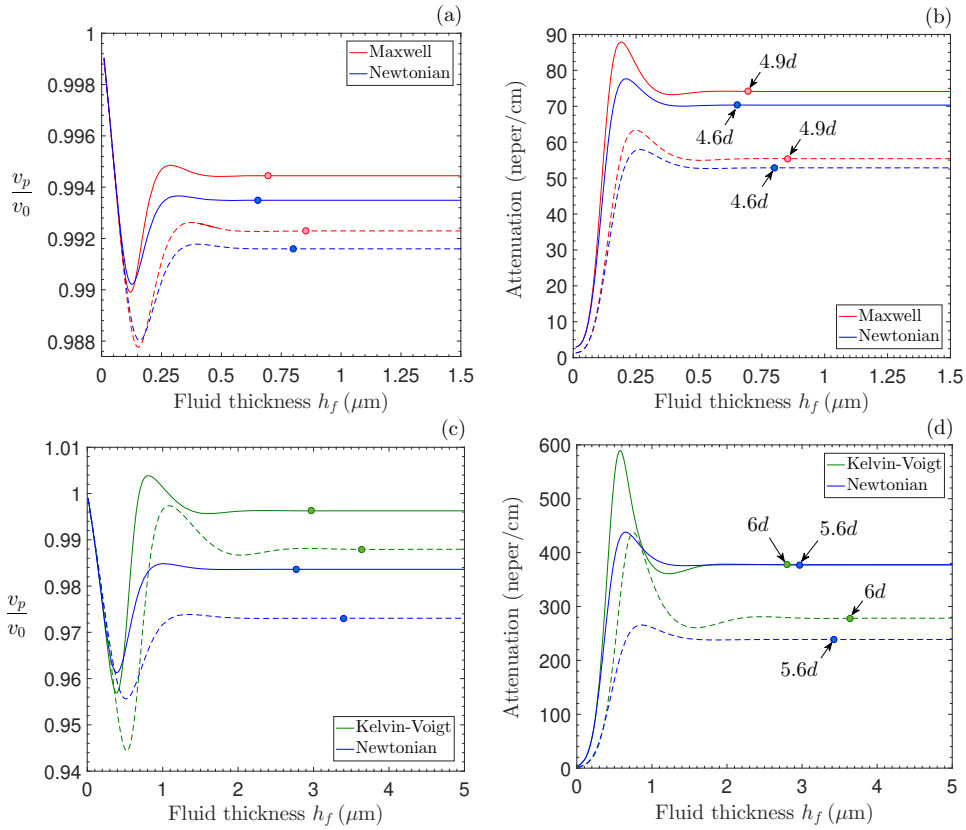

Figure 7: Phase velocity and attenuation versus fluid thickness with $\eta_v = 1 \times 10^{-3}\text{Pa} \cdot \text{s}$ and $h_v = 10\,\mu\text{m}$. Dashed lines $f = 100\,\text{MHz}$ and solid lines $f = 150\,\text{MHz}$. (a) and (b) $\chi = 62.1\%$; (c) and (d) $\chi = 88\%$. v_0 corresponds to the Love wave velocity without the fluid loading.

5. Conclusion

In this paper, Love wave propagation in viscoelastic waveguide loaded on its surface with viscoelastic fluids of finite thickness is investigated using an original approach based on the exact theory. A generalized analytical form of the complex dispersion equation was developed. Therefore, the curves highlighting the behavior of attenuation and phase velocity of Love waves as function of fluid thickness, operating frequency, glycerol concentrations and waveguide thickness were obtained. Five detailed dispersion equations were established, (i) viscoelastic waveguide and viscoelastic fluid with finite thickness, (ii) viscoelastic waveguide and semi-infinite viscoelastic fluid, (iii)

elastic waveguide and semi-infinite Maxwell fluid, elastic waveguide and semi-infinite Newtonian fluid, and viscoelastic waveguide without any fluid on its surface. The obtained generalized complex dispersion equation can be very useful in the design and optimization of Love wave fluid sensors.

Generally, the properties of the viscoelastic fluid can be described by a standard linear model, which predicts both the creep and stress relaxation behavior and, therefore, is applicable in the entire frequency range. An important contribution of this paper is the analysis of the impact of both waveguide viscosity η_v and the viscosity of fluid loading η on the Love wave velocity and attenuation. These characteristics of the Love wave dispersion curves in viscoelastic waveguide loaded with viscoelastic fluids are original and can be particularly useful in the design of biosensors and chemosensors based on the Love waves. From the performed analysis and numerical calculations, one can conclude that :

- Attenuation dispersion curves of the Love wave exhibit a maximum as a function of the waveguid thickness h_v. This is due to the energy confinement in the waveguide. For a given frequency, there exists a thickness for which the attenuation k_i attains the maximum, see 4. The amplitude of this maximum is amplified due to both the fluid viscosity and the viscosity of the waveguide.

- The change of the Love wave velocity and attenuation as a function of fluid thickness h_f of the loading fluid has the character of a damped sinusoid, for small initial values of the thickness h_f, see Figure 7. Overall it seems that taking in account the viscoelastic behaviour of the fluid amplifies its response in regard of its viscous behaviour.

- Dispersion curves of the phase velocity as a function of fluid thickness h_f, for frequencies 100 and 150 MHz, see Figure 7, show that the limiting thickness beyond which a Newtonian liquid can be treated as a semi-infinite can be safely assumed as $4.9d$ (4.9 times penetration depths into the liquid) for Maxwell model and $6d$ for Kelvin-Voigt model.

- To reasonably predict the characteristics responses of Love waves, the Maxwell fluid is more appropriate for low glycerol concentration and, the Kelvin-Voigt fluid is more suitable for high glycerol concentration and at high frequency. We can also observe that for low frequencies and

a low concentration of glycerol, we can approximate a material with a Maxwell's law of behavior as a Newtonian fluid and conversely for a high concentration of glycerol and high frequencies a Kelvin-Voigt fluid as a Newtonian fluid. Taking that in count modelling Newtonian behaviour will be less demanding in terms of calculation than viscoelastic models and it can be useful if we want to carry out a rapid simulation or to have sensors with a rapid response time.

This work is original contribution to the state of the art. Since it covers Love waves properties at both high (Kelvin-Voigt fluid) and low frequency (Maxwell fluid), the results obtained can be used in many fields of science and technology, such as: geophysics, non-destructive testing and in the design of viscosity sensors.

References

[1] D. Matatagui, J. L. Fontecha, M. J. Fernandez, I. Gracia, C. Cane, J. P. Santos and M. C. Horrillo. Love-Wave sensors combined with Microfluidics for fast detection of biological Warfare agents, *Sensors* **14**(7), 12658–69 (2014).

[2] F. Zhang, S. Li, K. Cao, P. Wang, Y. Su, X. Zhu and Y. Wan. A Microfluidic Love-Wave Biosensing Device for PSA Detection Based on an Aptamer Beacon Probe, *Sensors* **15**(6), 13839–13850 (2015).

[3] F. Josse, F. Bender and R. W. Cernose. Guided shear horizontal surface acoustic wave sensors for chemical and biochemical detection in liquids, *Analytical Chemistry* **73**(24), 5937–5944 (2001).

[4] M. I. G. Rocha, Y. Jimenez, F. A. Laurent and A. Arnau. Love Wave Biosensors: A Review, IntechOpen 277–310 (2013).

[5] K. Mitsakakis, A. Tsortos, J. Kondoh and E. Gizeli. Parametric study of SH-SAW device response to various types of surface perturbations, *Sensors and Actuators B: Chemical* **138**, 408–416 (2009).

[6] P. Kielczynski, M. Szalewski and A. Balcerzak. Effect of a viscous liquid loading onLove wave propagation, *International Journal of Solids and Structures* **49**(17), 2314–2319 (2012).

[7] A. El Baroudi. Influence of Poroelasticity of the Surface Layer on the Surface Love Wave Propagation, *Journal of Applied Mechanics* **85**, 051002-1–7 (2018).

[8] G. Kovacs and A. Venema. Theoretical comparison of sensitivities of acoustic shear wave modes for (bio) chemical sensing in liquids, *Applied Physics Letters* **61**(6) (1992).

[9] J. Du, G. L. Harding, J. A. Ogilvy, P. R. Dencher and M. Lake. A study of Love-wave acoustic sensors, *Sensors and Actuators A: Physical* **56** (3), 211–219 (1996).

[10] J. O. Kim. The effect of a viscous fluid on Love waves in a layered medium, *The Journal of the Acoustical Society of America* **91**(6), 3099–3103 (2014).

[11] S. Li, Y. Wan, C. Fan and Y. Su. Theoretical Study of Monolayer and Double-Layer Waveguide Love Wave Sensors for Achieving High Sensitivity, *Sensors* **17**(3) (2017).

[12] P. Kielczynski, M. Szalewski, A. Balcerzak and K. Wieja. Dispersion Curves of Love Waves in Elastic Waveguides Loaded with a Newtonian Liquid Layer of Finite Thickness, *Archives of Acoustics* **45**(1), 19–27 (2020).

[13] A. El Baroudi and J. Y. Le Pommellec. Viscoelastic fluid effect on the surface wave propagation, *Sensors and Actuators A* **291**, 188–195 (2019).

[14] P. Kielczynski. Surface Waves - New Trends and Developments, Properties and Applications of Love Surface Waves in Seismology and Biosensors, IntechOpen 17–31 (2018).

[15] B. A. Auld. Acoustic Fields and Waves in Solids, Volume 1, Wiley (1973).

[16] J. M. Carcione. Wave Fields in Real Media, 3rd Edition, elsevier (2015).

[17] A. El Baroudi and J. Y. Le Pommellec. Surface wave in a Maxwell liquid-saturated poroelastic layer, *Applied Acoustics* **159**, 107076 (2020).

[18] D. D. Joseph. Fluid Dynamics of viscoelastic liquids, Springer (1990).

[19] F. L. Guo and R. Sun. Propagation of Bleustein-Gulyaev wave in 6 mm piezoelectric materials loaded with viscous liquid, *International Journal of Solids and Structures* **45**(13), 3699–3710 (2008).

[20] R .R. Huilgol and N. P. Thien. Fluid Mechanics of Viscoelasticity, Volume 6, Elsevier Science (1997).

[21] C. Caliendo, S. Sait and F. Boubenider. Love-mode MEMS devices for sensing applications in liquids, *Micromachines* **7**(1), (2016).

[22] P. Kielczynski. Direct Sturm-Liouville problem for surface Love waves propagating in layered viscoelastic waveguides, *Applied Mathematical Modelling* **53**, 419–432 (2018).

[23] D. Chakraborty, E. V. Leeuwen, M. Pelton and J. E. Sader. Vibration of nanoparticles in viscous fluids, *Journal of Physical Chemistry C* **117**(16), 8536–8544 (2013).

[24] M. Pelton, D. Chakraborty, E. Malachosky, P. Guyot-Sionnest and J. E. Sader. Viscoelastic Flows in Simple Liquids Generated by Vibrating Nanostructures, *Physical Review Letters* **111**, 244502 (2013).

[25] A. El Baroudi. A note on the spheroidal modes vibration of an elastic sphere in linear viscoelastic fluid, *Physics Letters A* **384**, 126556 (2020).

[26] X. Yang, A. El Baroudi and J. Y. Le Pommellec. Analytical approach for predicting vibration characteristics of an embedded elastic sphere in complex fluid, *Archive of Applied Mechanics* **90**, 1399–1414 (2020).

[27] S. J. Martin, A. J. Ricco, T. M. Niemczyk, and G. C. Frye. Characterization of SH acoustic plate mode liquid sensors, *Sensors and Actuators* **20**(3), 253–268 (1989).

[28] P. B. Nagy and A. H. Nayfeh. Viscosity-induced attenuation of longitudinal guided waves in fluid-loaded rods, *The Journal of the Acoustical Society of America* **100**, 1501 (1996).